



Numerical investigation of air conditioning system configurations for achieving desired negative pressure in isolation rooms



Elaf S. Barrak^{a*}, Hasanain M. Hussain^b , Laith J. Habeeb^c 

^a Mechanical Engineering Dept., University of Wasit, Wasit -Iraq.

^b Mechanical Engineering Dept., University of Technology-Iraq, Alsina'a street, 10066 Baghdad, Iraq

^c Training and Workshop Center, University of Technology-Iraq, Baghdad, Iraq

*Corresponding author Email: me.20.16@grad.uotechnology.edu.iq

HIGHLIGHTS

- A novel airflow simulation studied AC inlet angle effects in an isolation room.
- Cassette AC units at different angles (0, 15, and 30 degrees) to protect respiratory patients and healthcare workers.
- Insights for healthier, more comfortable indoor environments were provided.
- Comprehensive inlet angle optimization for air quality management considering performance factors.

ARTICLE INFO

Handling editor: Sattar Aljabair

Keywords:

IAQ; Airborne infectious isolation room; contaminant distribution; CFD simulation; Tracer gas; CO₂.

ABSTRACT

This paper investigates a novel study about the influence of airflow simulation of an air conditioner (AC) inlet angle impacting negative pressure control in an airborne isolation indoor room (AIIR). The study focuses on four cassette Air Conditioner units set at different angles (0, 15, and 30 degrees) and their effect on air quality and airborne contamination removal for respiratory patients and healthcare workers by using computational fluid dynamics (CFD) simulations. Carbon dioxide is used as a tracer gas. The results showed that at a 0-degree angle, higher CO₂ concentrations were observed compared to inclinations of 15 and 30 degrees at three minutes. Inclinations of 15 and 30 degrees promote better air circulation with medium and high velocity, better Contaminant Removal Effectiveness (CRE), and better local Air Quality Index (LAQI), facilitating efficient dilution and dispersion of CO₂. In addition, these angles reflect the direction of airborne contamination to the side of the wall and keep them away from the healthcare workers, ensuring the medical staff's safety. In conclusion, The LAQI findings indicated an index value of 1.01 when measured at a 15-degree AC angle. In contrast, measurements taken at 0 and 30 degrees yielded values of 0.96 and 0.93, respectively, and the coefficient of restitution (CRE) exhibited values of approximately 100, 99.8, and 98 for AC angles of 15, 0, and 30 degrees, respectively, under low AC -velocity conditions.

1. Introduction

Humans have made efforts in an attempt to create indoor spaces that are comfortable for themselves. Negative pressure isolation rooms are crucial in preventing the spread of airborne contaminants or pathogens within healthcare facilities, laboratories, and other sensitive environments. The design and operation of air conditioning systems in these rooms are essential for maintaining the desired level of isolation and ventilation. While the angle of an air conditioner may not directly affect the isolation of negative pressure, other factors, such as the configuration of supply and exhaust openings, airflow patterns, and room sealing, significantly influence the system's effectiveness.

When evaluating the general pleasure of the environment, human health comes first. If the built environment is causing illness or detrimental to occupant health for whatever reason, this is cause for concern and could indicate a problem with the building system's design or technical operation. According to ASHRAE guidelines [1], there has been an increase in interest in both academic and practitioner literature on occupant health and building design because people spend between 80 and 90 percent of their time indoors, and studies have shown that a variety of comfort- and health-related effects are linked to characteristics of the building. SARS, or severe acute respiratory syndrome, recently posed a serious threat to the world at large. In terms of public health issues, COVID-19 is far worse than SARS (2003), Avian Influenza (2004), and H1N1 (2013) combined (2009). The world economy has seen its greatest recession since the Second World War, with more than 6 million lives lost [2]. One of the countries affected by the global coronavirus pandemic is Iraq. From February 24, 2020, in the city of Najaf, its appearance of 2020 has

been spread in Iraq. During the pandemic, 2.64 million cases and 25.4 thousand fatalities were associated with the coronavirus in Iraq [3]. With the effective creation of vaccines and the widespread use of immunization, we are steadily progressing in our fight against COVID-19. However, it has been noted in recent studies that additional viruses like COVID-19 will be transmitted to humans across animals as the global temperature environment changes [4]. There was a risk that a COVID-19-like illness would reappear in the future. Aerosols have been seen to be a significant COVID-19 transmission route [5,6]. Because the isolation ward has a greater control effect on the viral bioaerosols produced by patients' breathing patterns, COVID-19 patients can currently only be admitted and treated there [7]. However, the International Council of Nurses' inadequate numbers showed that over 90,000 healthcare workers (HCWs) were infected. Therefore, research into the effective removal of bioaerosols from isolation wards and the inhibition of their diffusion is essential to increase the safety of HCWs. Because indoor pollutants directly impact workers' health and well-being, it is critical to regulate indoor air quality (IAQ) in workplaces [8]. This is accomplished by installing heating, ventilation, and air conditioning (HVAC) systems in buildings to give residents comfortable temperatures and breathing air. These demands are met by supplying conditioned fresh air to control the environment's temperature and lower the concentration of pollutants [9].

The COVID-19 outbreak is challenging and severely influences people's quality of life due to the virus's adverse impacts on human health and other difficulties, such as the increasing incidence of poverty, the global financial crisis, and the job crisis. COVID-19 poses a significant risk to patients with preexisting illnesses since it may enter the upper-lower respiratory system and cause lung infections and chronic obstructive pulmonary disease. The virus's virulence, environmental sustainability, and longevity are all factors that will contribute to its global spread in the next years [10,11]. To combat the COVID-19 outbreak, numerous medical, social, and engineering measures have been suggested. These include approaches for treatment, prevention, detection, and prediction [11]. The burden of pathogens emitted indoors can be reduced and infections among occupants can be avoided with the help of engineering and architectural solutions. Experts are debating how to use effective ventilation and air disinfection methods to restrict the spread of COVID-19 in interior settings now that they have a better grasp of the virus [12]. Health consequences, route of viral departure from the body, concentration, and particle size distribution of the aerosol carrying the virus; the environment's physical features (temperature, humidity, oxygenation, UV light, suspension medium, etc.); the pattern of air circulation; and the presence or absence of biological contaminants, such as viruses, in the environment [13,14]. All these elements show how crucial it is to maintain indoor air quality that is at least as good as outdoor air in terms of pathogen removal and perceived cleanliness. However, most of our indoor workplaces are not built to stop the transmission of airborne infections.

Currently, there is a lot of scientific research on COVID-19, particularly for public health interventions and engineering methods for enhancing IAQ. Table 1 shows a summary of the previous studies with different specific conditions. The isolation ward mostly prevented contaminants from flowing out by regulating the pressure differential between the wards.

Prior studies lacked specific emphasis on air conditioning configurations, provided limited quantitative data, frequently lacked validation in real-world scenarios, neglected the variability in room geometry, and primarily focused on individual contaminants. The static system assumptions were frequently employed, while the advanced filtration systems were often given insufficient emphasis. This paper presents a numerical study investigating various air conditioning system configurations and their numerical implications for achieving the desired negative pressure in isolation rooms. By analyzing the numerical data and considering the interplay of key parameters, this study aims to provide insights into optimizing the design and operation of air conditioning systems to enhance isolation effectiveness and ventilation in negative pressure rooms. This work aims to provide the findings of numerical research conducted at the University of Technology to investigate the behavior and features of a real space. The research aims to acquire insights into many characteristics of space, such as its airflow patterns, temperature distribution, and air quality, by applying computer models and simulations.

2. Numerical study

CFD simulation, which can thoroughly analyze the spatial airflow and the spread of contamination, was used to analyze how the airborne contamination spread in isolation rooms based on the types and locations of the supply air diffuser and exhaust air diffuser.

By quantitatively analyzing the numerical data, this study provides insights into effective strategies for mitigating CO₂ levels, optimizing ventilation systems, and enhancing occupant comfort and well-being in indoor environments. The numerical work is based on assumptions in the present study, the following assumptions were made:-

1. Transient flow.
2. Three dimensional.
3. Newtonian fluid.
4. Incompressible fluid.
5. Neglect radiation heat transfer.

Table 1: A summary of previous studies

Space of study	Case study	Conclusion	Ref.
Bedroom.	Air purifying respirators with or without HEPA filtration.	Positive effects of filtration require substantial exposure contrasts, especially in the bedroom, and possibly not confounding by drug intake or existing disease.	[15]
Cars.	AC operation modes.	Human subjects' HRV indices during the commute are affected by PM2.5 in the automobile, although using the AC may enhance air quality and mitigate these effects.	[16]
Room.	Three ventilation MV, One and two-slot POV	The decreased air velocity distribution may increase the patient's exposure to various indoor airborne pollutants during orthopedic surgery.	[17]
Office room.	Comparison between AC types.	The 4-way cassette is better than MV AC.	[18]
Office room.	Indoor air disturbance with the conventional Mixing Ventilation system.	The walking disturbance deteriorated the efficiency of personalized ventilation (P.V.), and the safe distance was 0.85 cm.	[19]
Operating room.	4 different cases were examined with a real person and a thermal Manikin.	The decreased air velocity distribution may increase the patient's exposure to various indoor airborne pollutants during orthopedic surgery.	[20]
Hospital.	Three engineering strategies.	The "low-level extraction" technique of ventilation systems effectively removes pollutants.	[21]
Full-scale room.	Comparison of adaptive and ceiling ventilation	A ceiling or upper sidewall air supply and adaptive wall-based attachment ventilation result in a 15% - 47% lower average concentration of contaminants.	[22]
A ventilated room.	Three angles of AC gate 0°, 30°, and 60°	Increasing the AC inlet gate angle leads to flow distribution in the room with weak vortices.	[23]
Hospitals.	Various ventilation strategies were designed.	Pollutant removal was greatly influenced by the position of the exit; however, increased ventilation alone does not necessarily enhance air dispersion.	[24]

2.1 Geometry model and mesh generation

Geometry modeling and mesh generation are fundamental steps in numerical simulations and computational modeling across various scientific and engineering disciplines. Geometry modeling involves creating a virtual representation of the real-world object or system under study. It encompasses defining the domain's shape, size, and geometric features. Mesh generation, on the other hand, involves dividing the geometric domain into smaller, interconnected elements or cells to facilitate numerical calculations.

This study used a three-dimensional model of the isolation room, as shown below in Figure 1. The room was drawn using the Solidworks 2022 package. For the numerical simulations, it is very necessary to have a precise representation of the room's geometry and an adequate creation of the mesh. The domain is partitioned into smaller pieces during the mesh creation to assist numerical computations. The geometry model accurately represents the space's size, shape, and characteristics. These processes guarantee that the simulation results are as accurate and faithful as possible.

The dimension of the isolation room is 3.5 m×3 m×2.75 m. The air conditioner device has two parts (inlet and outlet unit). The inlet ventilation part is 0.3 m ×0.25 m in the upper part of the east wall, and the outlet dimension is 0.3 m×0.2 m in the lower opposite wall. The 4-way air supply cassette AC of (0.6 m×0.6 m) is located in the middle ceiling of the top wall, which was used to perform better than typical AC [18]. Two fluorescent lamps of 1 m are in the ceiling beside the AC. The patient body model of 170 cm in height and 78 kg weight with a realistic human head geometry containing full facial features was employed, and the mouth size is (0.02 m×0.02 m). The air conditioner (AC) dimension is (0.6 m×0.6 m) with three gate angles (0°, 15°, and 30°) in the center of the roof of the isolation room, as shown in Figure 1. The air velocity exiting the air conditioner (AC) is divided into 3 levels (low speed, medium speed, high speed) considered in the study. The relevant parameter in the numerical calculation is shown in Table 2. The airborne indoor isolation room is described in Figure 2.

This study uses a tetrahedral mesh to achieve satisfactory convergence for a more accurate mesh and result. The total number of elements is approximately 1.32 million with medium smoothing, which seems sufficient for a reasonable resolution of the flow field by using mesh. Fluent meshing is used due to the complex geometry model and unstructured grids around the human body, as shown in Figure 3. To predict high resolution, the unstructured mesh was chosen for the volume domain with refined mesh in front of the human body. Mesh quality and statistics are target skewness 0.9, max: cell length 0.05 m, mesh quality 0.2, and growth size 1.2.



Figure 1: The indoor unit of a ceiling-type air conditioner [25]

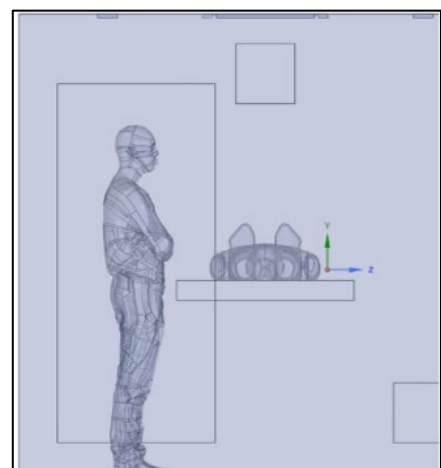
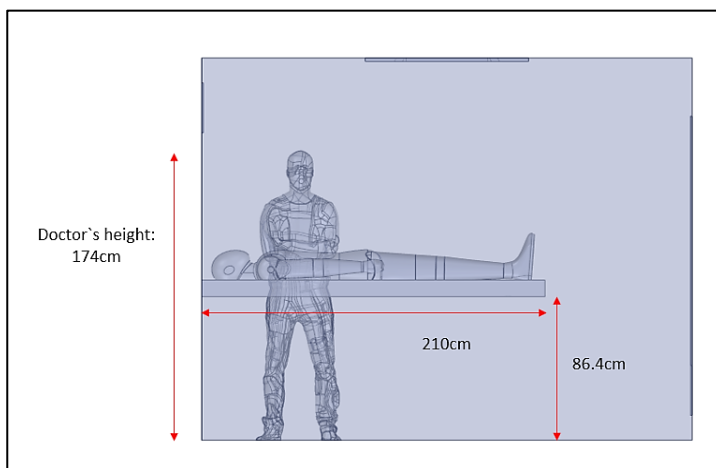
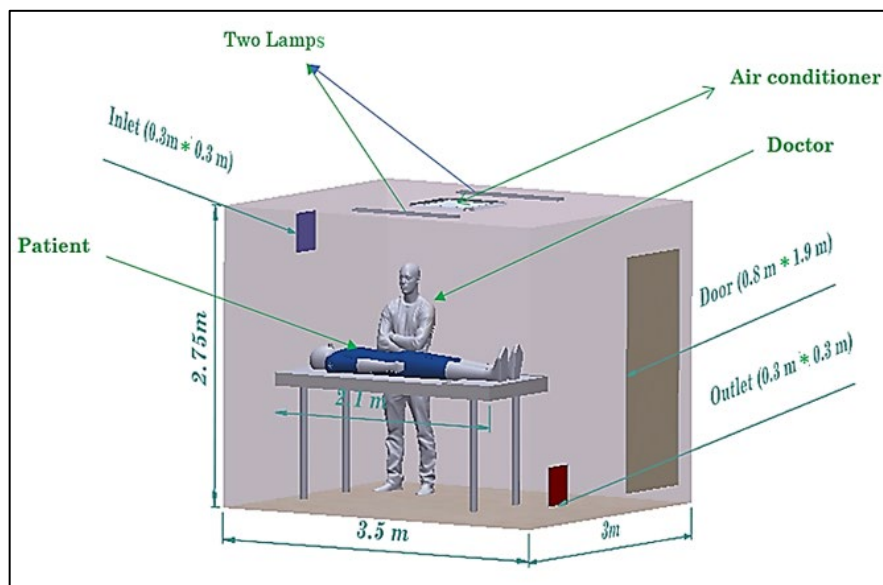


Figure 2: Geometric model of the operating room showing the isolation room ventilation

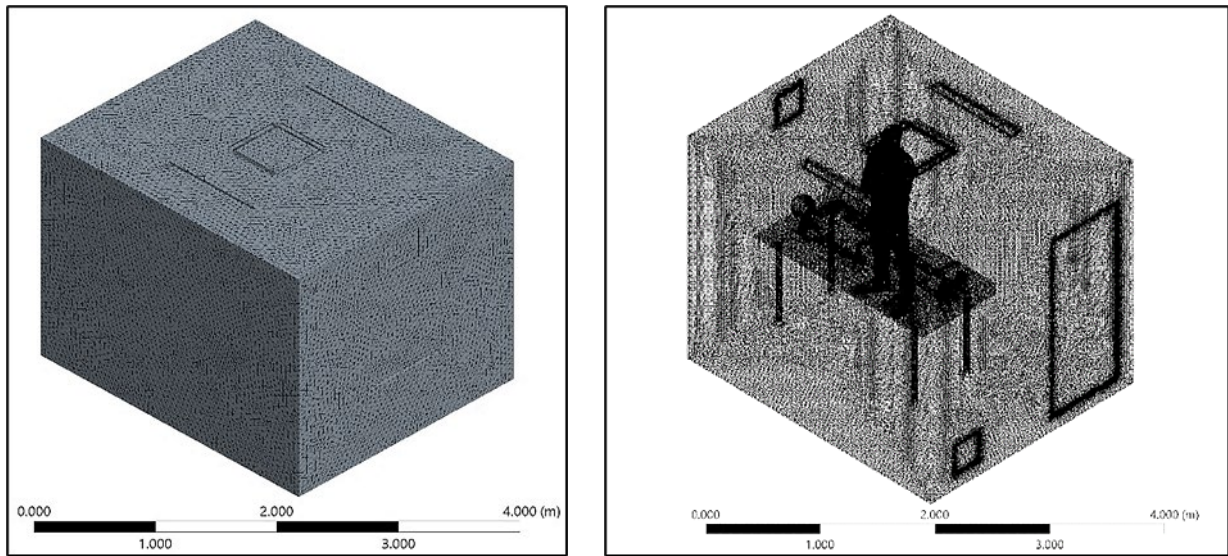


Figure 3: Mesh generation of the computational domain

Figure 4 shows the AC inlet angle. The numerical relation between the angle of an air conditioner and the isolation of negative pressure in a room would depend on various factors, including the design and specifications of the air conditioning system, the room size, the airflow rate, and the desired level of negative pressure [26-28]. Table 2 shows the three cases that were investigated as follows:

Table 2: Case studies

Case number	θ (deg.)	Air Conditioner Volume Flowrate (CFM)
1	0°	Low speed
2	0°	Medium speed
3	0°	High speed
4	15°	Low speed
5	15°	Medium speed
6	15°	High speed
7	30°	Low speed
8	30°	Medium speed
9	30°	High speed

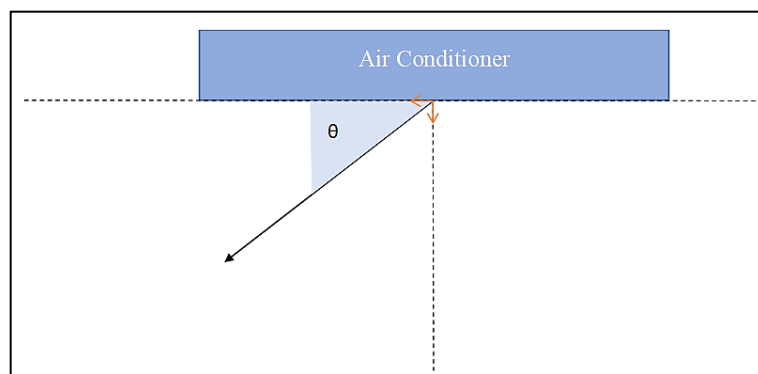


Figure 4: AC inlet gate angle

2.2 Tracer gas study CO₂

Carbon dioxide, sometimes known as CO₂, is a naturally occurring gas that is an essential component of our planet's atmosphere. However, increased CO₂ levels may have detrimental impacts on the health and well-being of humans when they are found in enclosed situations. To maintain a healthy and pleasant indoor environment, it is necessary to have a solid understanding of the behavior and distribution of CO₂ as an interior gas. This article summarizes the findings of computational research that aimed to investigate the dynamics of carbon dioxide CO₂ as an internal gas in various indoor situations.

The numerical analysis will consider ventilation rates, room dimensions, and air circulation patterns. The study will examine the influence of these factors on the buildup and distribution of CO₂, helping to identify potential areas of concern and areas for improvement in indoor air quality management. The present study used CO₂ as a tracer gas instead of aerosol particles because it was more reliable and effective in previous studies [29]. Some papers used other gases, such as N₂O [30] and SF₆ [19].

2.3 Governing equations

The thermal and flow fields are simulated numerically, solving the stable turbulent Navier-Stokes and energy equations using the Finite Volume Method (FVM), including the continuity equation.

Thus, the Reynolds-averaged Navier-Stokes (RANS) technique was used to represent the unsteady flow and is often used to solve the airflow field. Because of its reliability in forecasting airflow fields across solid bodies, the RNG k-ε model with improved wall treatment was used [31–33]. In addition, it performs well in room ventilation [34]. A three-dimensional transient study was selected for modeling in this case. This model was used in the study of [35,17,36]. The SIMPLE algorithm is used to couple the pressure and velocity. A power law scheme was adopted for momentum equation and energy equation discretization. The momentum, energy, and k-ε equations were discretized using the second-order upwind scheme, while the transient term was discretized using the second-order implicit scheme. As for pressure, the “PRESTO!” scheme was used since it accounts for pressure gradients at the boundaries [19,37]. The transient evolutions of the air velocity, air temperature, and CO₂ concentration are simulated. The general equation becomes as below:

2.3.1 Conservation of mass: continuity equation

Equation 1 can be expressed mathematically for an incompressible fluid as:

$$\frac{\partial u}{\partial x} + \frac{\partial v}{\partial y} + \frac{\partial w}{\partial z} = 0 \quad (1)$$

where: u , v and w are the velocity corresponding of three components to the x , y and z directions, respectively.

2.3.2 Conservation of momentum: momentum equation of newton's

Second Law

Equation 2 in x -direction

$$\frac{\partial(\rho u)}{\partial t} + \frac{\partial(\rho uu)}{\partial x} + \frac{\partial(\rho uv)}{\partial y} + \frac{\partial(\rho uw)}{\partial z} = -\frac{\partial p}{\partial x} + \mu \left[\frac{\partial^2 u}{\partial x^2} + \frac{\partial^2 u}{\partial y^2} + \frac{\partial^2 u}{\partial z^2} \right] \quad (2)$$

Equation 3 in y -direction

$$\frac{\partial(\rho v)}{\partial t} + \frac{\partial(\rho uv)}{\partial x} + \frac{\partial(\rho vv)}{\partial y} + \frac{\partial(\rho vw)}{\partial z} = -\frac{\partial p}{\partial y} + \mu \left[\frac{\partial^2 v}{\partial x^2} + \frac{\partial^2 v}{\partial y^2} + \frac{\partial^2 v}{\partial z^2} \right] + S_{bj} \quad (3)$$

Equation 4 in z -direction

$$\frac{\partial(\rho w)}{\partial t} + \frac{\partial(\rho uw)}{\partial x} + \frac{\partial(\rho vw)}{\partial y} + \frac{\partial(\rho ww)}{\partial z} = -\frac{\partial p}{\partial z} + \mu \left[\frac{\partial^2 w}{\partial x^2} + \frac{\partial^2 w}{\partial y^2} + \frac{\partial^2 w}{\partial z^2} \right] \quad (4)$$

2.3.3 Conservation of energy

Mass, energy, and momentum are constant values within a closed system. The first law of thermodynamics states that everything that enters is equivalent to something from the system in Equation 5 [38].

$$\rho \frac{\partial}{\partial x}(uT) + \rho \frac{\partial}{\partial y}(vT) + \rho \frac{\partial}{\partial z}(wT) = \frac{\partial}{\partial x}(\Gamma_{eff,h} \frac{\partial T}{\partial x}) + \frac{\partial}{\partial y}(\Gamma_{eff,h} \frac{\partial T}{\partial y}) + \frac{\partial}{\partial z}(\Gamma_{eff,h} \frac{\partial T}{\partial z}) + S_T \quad (5)$$

2.3.4 Transport equation

The turbulence kinetic energy, k , and its rate of dissipation, ε , are obtained from the following transport equations below:

$$\frac{\partial}{\partial x}(\rho uk) + \frac{\partial}{\partial y}(\rho vk) + \frac{\partial}{\partial z}(\rho wk) = \frac{\partial}{\partial x}(\frac{\mu t}{\sigma_k} \frac{\partial k}{\partial x}) + \frac{\partial}{\partial y}(\frac{\mu t}{\sigma_k} \frac{\partial k}{\partial y}) + \frac{\partial}{\partial z}(\frac{\mu t}{\sigma_k} \frac{\partial k}{\partial z}) + G_K - \rho \varepsilon \quad (6)$$

And

$$G_K = \mu t [2((\frac{\partial u}{\partial x})^2 + (\frac{\partial v}{\partial y})^2 + (\frac{\partial w}{\partial z})^2) + (\frac{\partial u}{\partial y} + \frac{\partial v}{\partial x})^2 + (\frac{\partial u}{\partial z} + \frac{\partial w}{\partial x})^2 + (\frac{\partial v}{\partial z} + \frac{\partial w}{\partial y})^2] \quad (7)$$

The ε transport equation is given by:

$$\frac{\partial}{\partial x}(\rho u \varepsilon) + \frac{\partial}{\partial y}(\rho v \varepsilon) + \rho \frac{\partial}{\partial z}(\rho w \varepsilon) = \frac{\partial}{\partial x}(\frac{\mu t}{\sigma_k} \frac{\partial \varepsilon}{\partial x}) + \frac{\partial}{\partial y}(\frac{\mu t}{\sigma_k} \frac{\partial \varepsilon}{\partial y}) + \frac{\partial}{\partial z}(\frac{\mu t}{\sigma_k} \frac{\partial \varepsilon}{\partial z}) + (C_1 G_K - C_2 \rho \varepsilon) \frac{\varepsilon}{k} \quad (8)$$

$\sigma_k, \sigma_\varepsilon, C_1, C_2, C_3, C_\mu$ are the constants of the turbulent model given in Table 3.

Table 3: Constants of the standard k- ε model

σ_k	σ_ε	$C_1\varepsilon$	$C_2\varepsilon$	C_μ
1.0	1.3	1.44	1.92	0.09

2.3.5 Modeling the turbulent viscosity

The turbulent (or eddy) viscosity, μ_t , is computed as equation follows:

$$\mu_t = \frac{C_D \rho K^2}{\varepsilon} \quad (9)$$

where C_D is an empirical constant, turbulence is defined as irregular velocity in equation below [19].

$$K = \frac{1}{2} \sqrt{u^2 + v^2 + w^2}$$

2.4 Contaminant removal effectiveness

Contaminant Removal Effectiveness (CRE) refers to the efficiency or effectiveness of a system or method in removing contaminants from a given environment. It quantifies the ability of a ventilation system, air purification device, or other engineering control measures to eliminate or reduce the concentration of contaminants in a specific space [34,39,40]

CRE is typically expressed as a percentage or decimal value between 0 and 1. A CRE of 1 indicates that the system can completely remove the contaminants, resulting in an equilibrium state with no further increase in concentration. On the other hand, a CRE below 1 signifies that the system cannot remove contaminants efficiently, leading to an increase in the concentration of the contaminants over time [41].

The calculation of CRE involves comparing the initial concentration of the contaminant with the concentration after the implementation of the control measure or system. The difference between the two concentrations is used to determine the effectiveness of the system in removing the contaminants, as shown in the equation below [42,43]:

$$\varepsilon = \frac{C_e - C_s}{C_b - C_s} \quad (10)$$

The letters C_e , C_s , and C_b represent the contaminant concentrations at the exhaust, supply, and average contaminant concentrations in the respiratory zone (1.3–1.7 m above the floor). CRE can be influenced by various factors, such as the efficiency of the control measure, airflow rates, filtration capabilities, and the contaminants' characteristics. It is an important parameter to consider when evaluating the performance of ventilation systems, air purifiers, or other engineering measures to improve indoor air quality and reduce exposure to harmful substances. By quantifying the effectiveness of contaminant removal, CRE provides valuable information for designing and selecting appropriate control measures to mitigate the impact of contaminants on human health and create healthier indoor environments [44].

2.5 Local air quality index

The Local Air Quality Index (LAQI) is a gauge for air quality in a given location. A numerical value or rating is provided to indicate the overall air quality and the possible health concerns connected with air pollutants present in that location.

Typically, the index is broken down into subcategories, such as "Good," "Moderate," "Unhealthy," "Very Unhealthy," and "Hazardous," to provide a more nuanced picture of the air quality. A LAQI value of 1 represents a system where the air is perfectly mixed, indicating efficient ventilation and removal of polluted air from that specific location. Conversely, a higher LAQI value indicates a better ability of the ventilation system to effectively expel contaminated air from that particular point [24,44].

$$LAQI = \frac{C_e}{C} \quad (11)$$

C_e represents the average mass fraction of the contamination flowing outside the computational domain and C represents the mass fraction of the contaminant present at a particular site. It is important to note that the specific calculation and interpretation of the LAQI index may vary across different regions and countries, as it can be customized to suit local air quality monitoring programs and standards [34].

2.5.1 Boundary conditions and model validation

Firstly, the transient evolutions of the air velocity, air temperature, and CO_2 concentration are simulated. For the system airborne infectious isolation rooms (AIIR), according to the standard ASHRAE, the negative pressure difference must be maintained to reduce the airborne contaminant disease, and it was set at Pa at the outlet. In addition, it was assumed that the walls are adiabatic, with no heat transfer or storage within. The detailed boundary conditions used in the CFD method are summarized in Table 4 and Table 5.

Table 4: Boundary conditions of the CFD method

Boundary surfaces	Boundary conditions
Analysis type	Transient solution with time step (0.1 s).
Air conditioner	4-way Air Supply cassette AC with different inlet angles $\theta = (0^\circ, 15^\circ \text{ and } 30^\circ)$ (Figure 4), Temperature = 18°C .
Air supply	Volume flowrate inlet= (600, 671, and 742) CFM, Temperature = 20°C .
Air exhaust	Pressure outlet.
Wall/ceiling/floor/bed	Boundary wall, adiabatic.
Ceiling lamp	The wall boundary has a constant heat flux for each one, 40 W/m^2 .
Mouth	
Tracer gas	CO_2 gas.
Temperature	34.0°C [39].
Breathing profile	UDF, turbulence intensity 10%,

Table 5: Occupants and equipment's heat load summary

Item	No.	Power (W)
Person	2	80 W per person
Lamp	2	40 W per one

3. Results and discussion

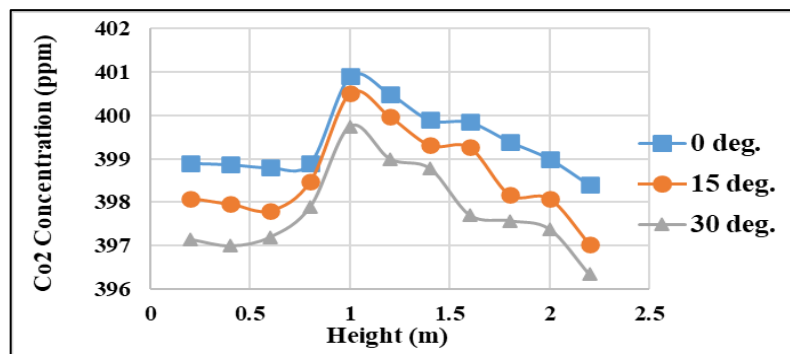
3.1 Contaminant distribution with patient's breathing

The current study investigated the distribution, concentration levels, and movement patterns of carbon dioxide (CO_2) within different settings, such as workplaces, schools, and residential structures. The following physical results and discussions were observed:

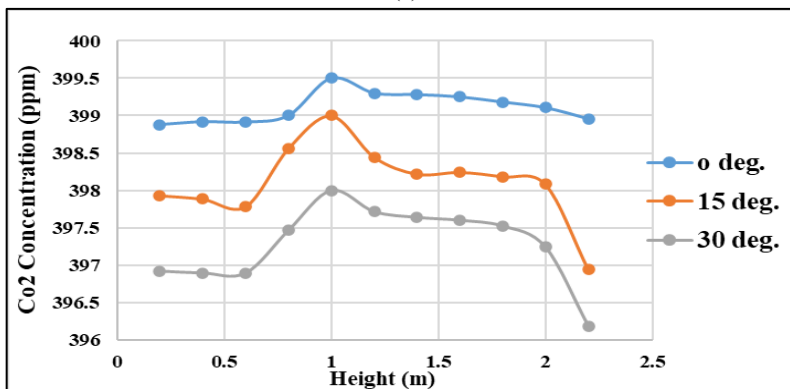
- 1) Exhaled CO_2 settles towards the ground: Figure 5 (a), (b) and (c) shows that exhaled CO_2 tends to settle at low, medium, and high speeds, respectively. This suggests that the CO_2 content may stay relatively constant at lower elevations. This phenomenon is commonly observed in confined spaces with inadequate ventilation.
- 2) Concentration of CO_2 decreases with increasing distance from the floor: As the distance from the floor increases, the concentration of CO_2 decreases. The CO_2 concentration is lowest near the occupants' breathing zone, typically around 1.3-1.5 meters above the floor. This attenuation in CO_2 concentration is influenced by airflow patterns, ventilation systems, and natural convection as shown in Figure 6, a front-view depiction of breathing contaminant distribution in the breathing zone is presented at zero degrees, showcasing three distinct inlet speeds: (a) low speed, (b) medium speed, and (c).
- 3) Buoyancy effects and temperature differences contribute to CO_2 rise near the ceiling: Due to buoyancy effects and temperature differences in the room, CO_2 may rise again near the ceiling, contributing to its buildup. Insufficient ventilation or inadequate dispersion of airflow in elevated locations can contribute to the accumulation of carbon dioxide (CO_2). This phenomenon is illustrated, Figure 7 which illustrated the breathing contaminant distribution at the breathing zone at 15 degrees, featuring three different inlet speeds: (a) low speed, (b) medium speed, and (c) high speed. Additionally, Figure 8 portrays the breathing contaminant distribution at the breathing zone at 30 degrees, displaying three distinct inlet speeds: (a) low speed, (b) medium speed, and (c) high speed. This visual representation provides a comprehensive view of the spatial distribution of contaminants in the breathing zone under varying inlet speeds and angles, offering valuable insights into the dynamics of contaminant dispersion within the examined environment.
- 4) Room variables influence CO_2 behavior: Factors such as room size, ventilation system design, occupant activities, and the placement and angle of the air conditioner can affect how CO_2 behaves in a given space. Poor ventilation or airflow patterns due to inadequate architecture can result in CO_2 buildup near the ground.
- 5) AC unit angle affects CO_2 dispersion: When the air conditioner is positioned at a zero-degree angle as shown in figure 9 which represent a top view of breathing contaminants at zero degrees AC angle featuring three different inlet speeds (a)low speed, (b) medium speed and (c) high speed, poor ventilation and airflow close to the ground can cause CO_2 to become stagnant, leading to its buildup. CO_2 is heavier than air and tends to sink to lower elevations. When the inclination angle increase as shown in the top plane in Figure 10 and 11, which illustrates the impact of varying AC inclination angles (15° , and 30°) the CO_2 concentration was in the direction away from Health Care Worker (HCW) which offers more protection to health care workers and decreasing with increasing AC inlet speed as shown in (a),(b) and (c). The figure provides a visual representation of the different scenarios denoted by the combinations of AC inclination angles and airflow speeds, labeled as a, b, and c, respectively. The concentration of CO_2 may rise near the ground without sufficient ventilation or a breeze to carry it away.
- 6) AC unit angle and airflow velocity correlation: Decreasing the angle of the air conditioner increases the airflow velocity, and vice versa. When the unit is tilted at a small angle, the airflow is most downwardly directed, resulting in greater mixing and dispersion of CO_2 near the floor. The airflow may be dispersed more widely at steeper angles, potentially slowing it down and leading to CO_2 buildup near the floor.

- 7) Balancing AC unit tilt and speed for optimal airflow and CO₂ dispersion: To achieve better air mixing and reduced CO₂ concentrations near the floor, there needs to have an appropriate balance between the angle and airflow velocity of the air conditioner. Adjusting these parameters to meet the space's and its occupants' needs can enhance airflow and CO₂ dispersion.
- 8) AC inlet angle and CO₂ dispersion: Figures 6,7 and 8 illustrate the frontal perspectives of air conditioning (AC) units positioned at inclination angles of 0°, 15°, and 30°, respectively. These figures showcase three distinct airflow speeds: low, medium, and high, denoted as a,b and c, respectively. These visual representations provide a comprehensive depiction of the combined effects of AC inclination angles and airflow speeds on the distribution and movement of air from the AC units which showed that the CO₂ concentration is greater when four cassette AC units are arranged at a 0-degree angle compared to 15 and 30-degree inclinations. Tilting the AC units between 15 and 30 degrees allows for more diffuse and uniform airflow around the room, resulting in easier dilution and dispersion of CO₂.
- 9) AC inlet angle and protection of healthcare workers: A 15-degree AC inlet angle was found to optimize the ventilation system's ability to create a "protected zone" around healthcare workers. By directing the airflow towards the sidewalls, this angle prevents airborne contaminants, including CO₂, from accumulating in the breathing zone of healthcare workers. This design strategy reduces the risk of infection transmission, particularly in isolation rooms and healthcare settings where infectious diseases pose a significant risk.

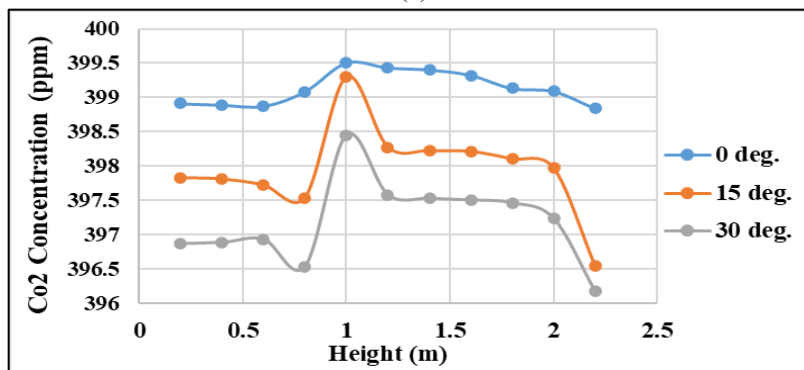
The current study's findings contribute to the development of evidence-based guidelines and recommendations for maintaining healthy indoor air quality standards, particularly in terms of CO₂ distribution, concentration, and movement patterns.



(a)



(b)



(c)

Figure 5: The relationship between Co₂ concentration and room height at three different inlet angles and three different inlet speeds: (a) low speed, (b) Medium speed, and (c) high speed

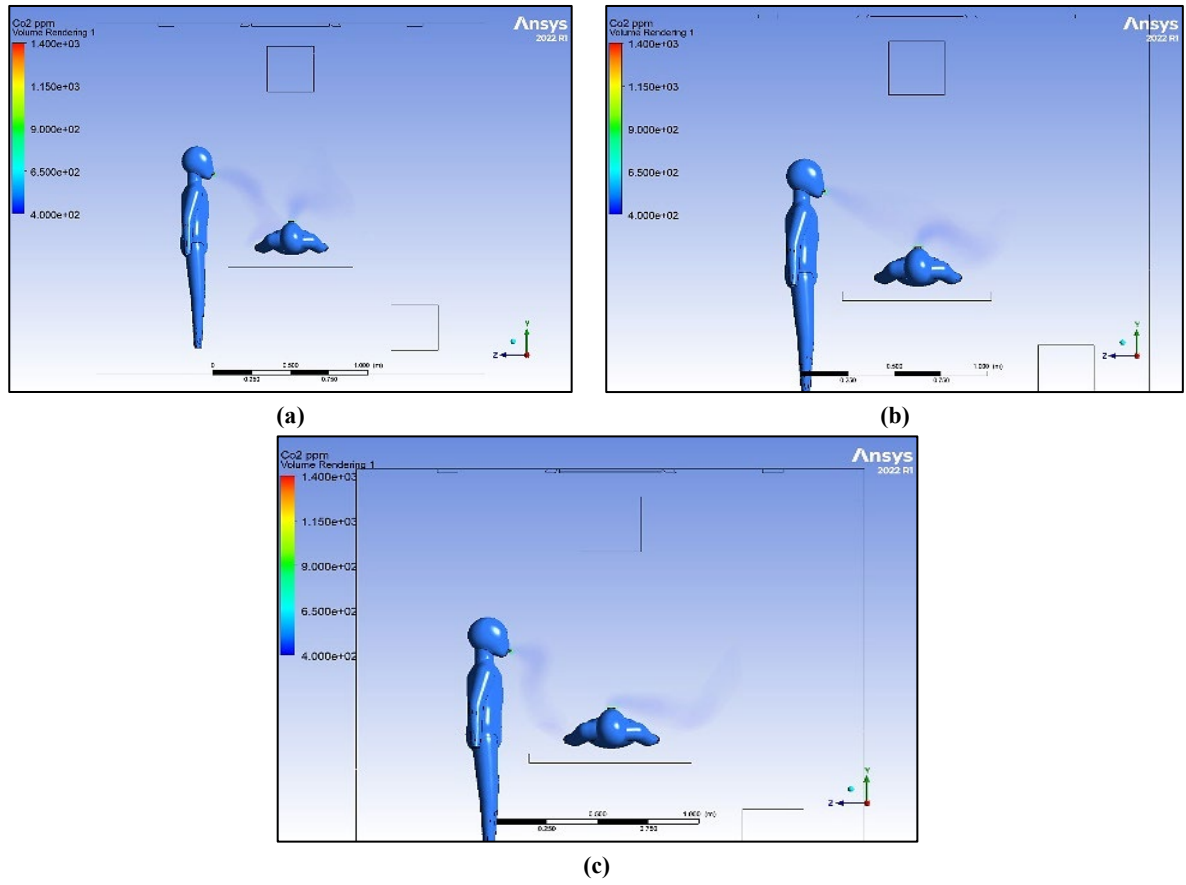


Figure 6: Illustrates a front view of breathing contaminant distribution in the breathing zone at zero deg, at three different inlet speeds: (a) low speed, (b) medium speed, and (c) high speed

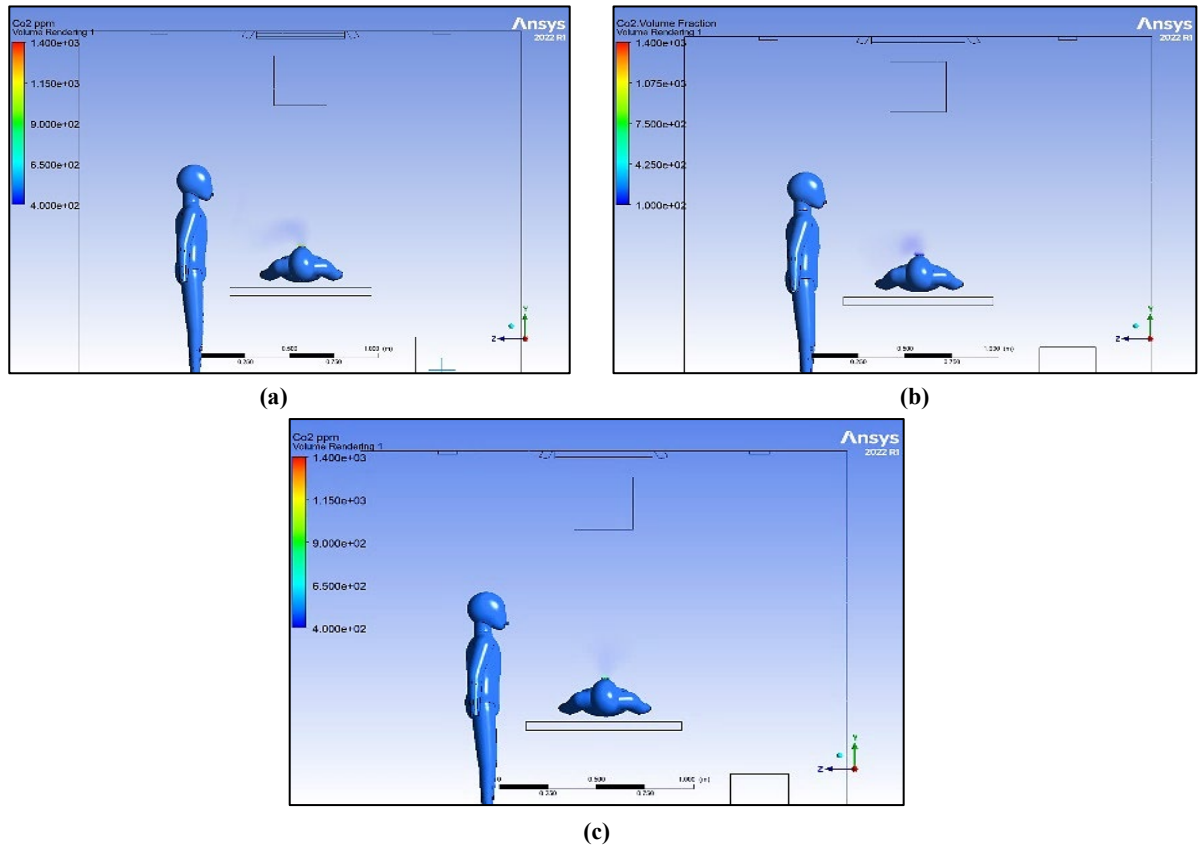


Figure 7: Illustration of a front view breathing contaminant distribution at the breathing zone at 15 deg, at three different inlet speeds: (a) low speed, (b) medium speed, and (c) high speed

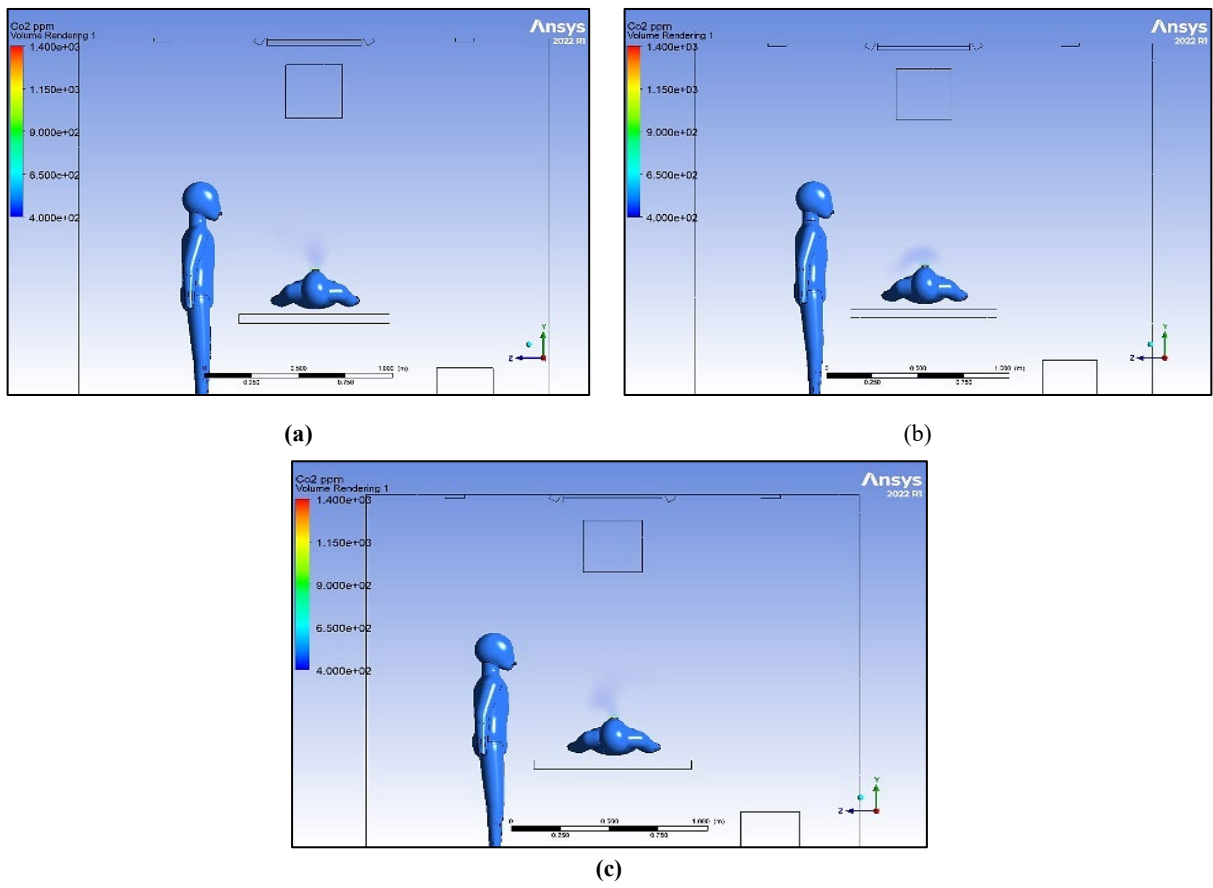


Figure 8: Illustration of a front view breathing contaminant distribution at the breathing zone at 30 deg, at three different inlet speeds: (a) low speed,(b) medium speed, and (c) high speed

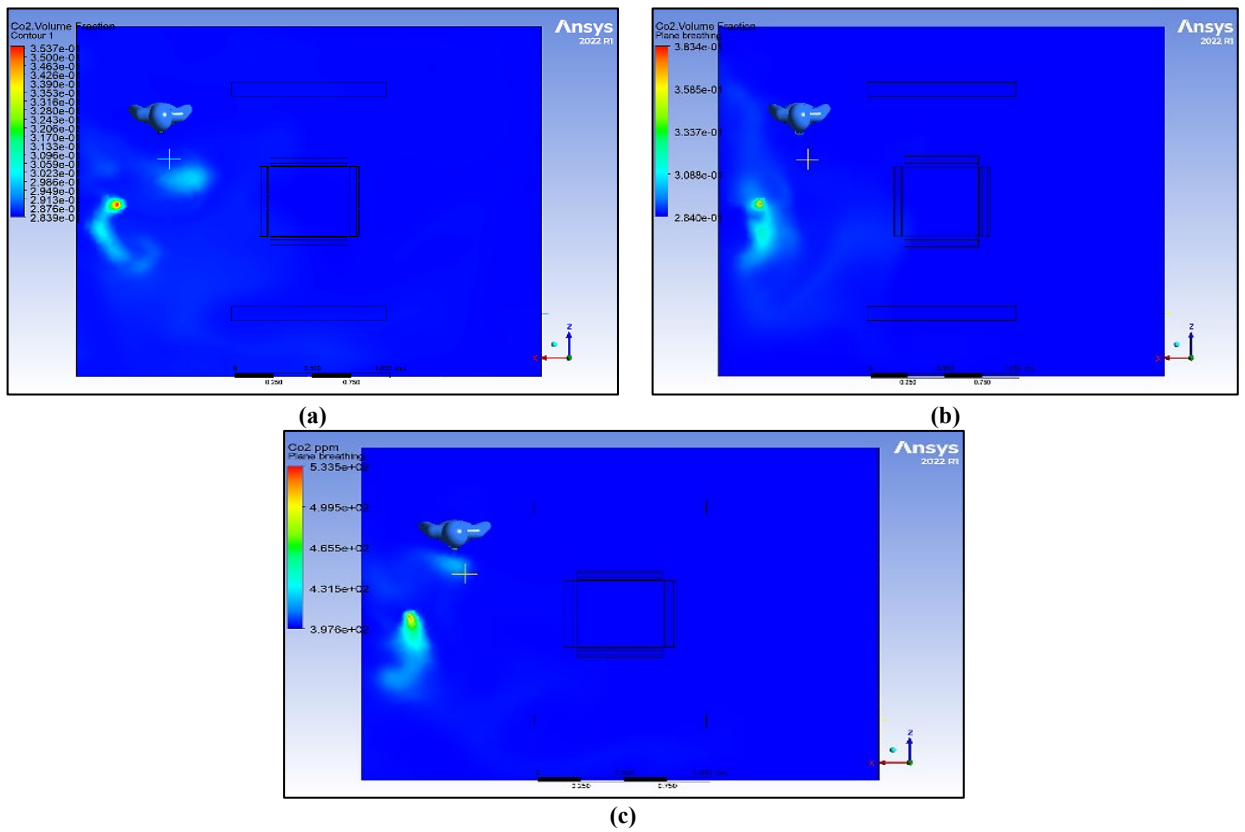


Figure 9: Illustration of a top view of breathing contaminant distribution at the breathing zone at zero deg. AC inclination angle at three different inlet speeds: (a) low speed, (b) medium speed, and (c) high speed

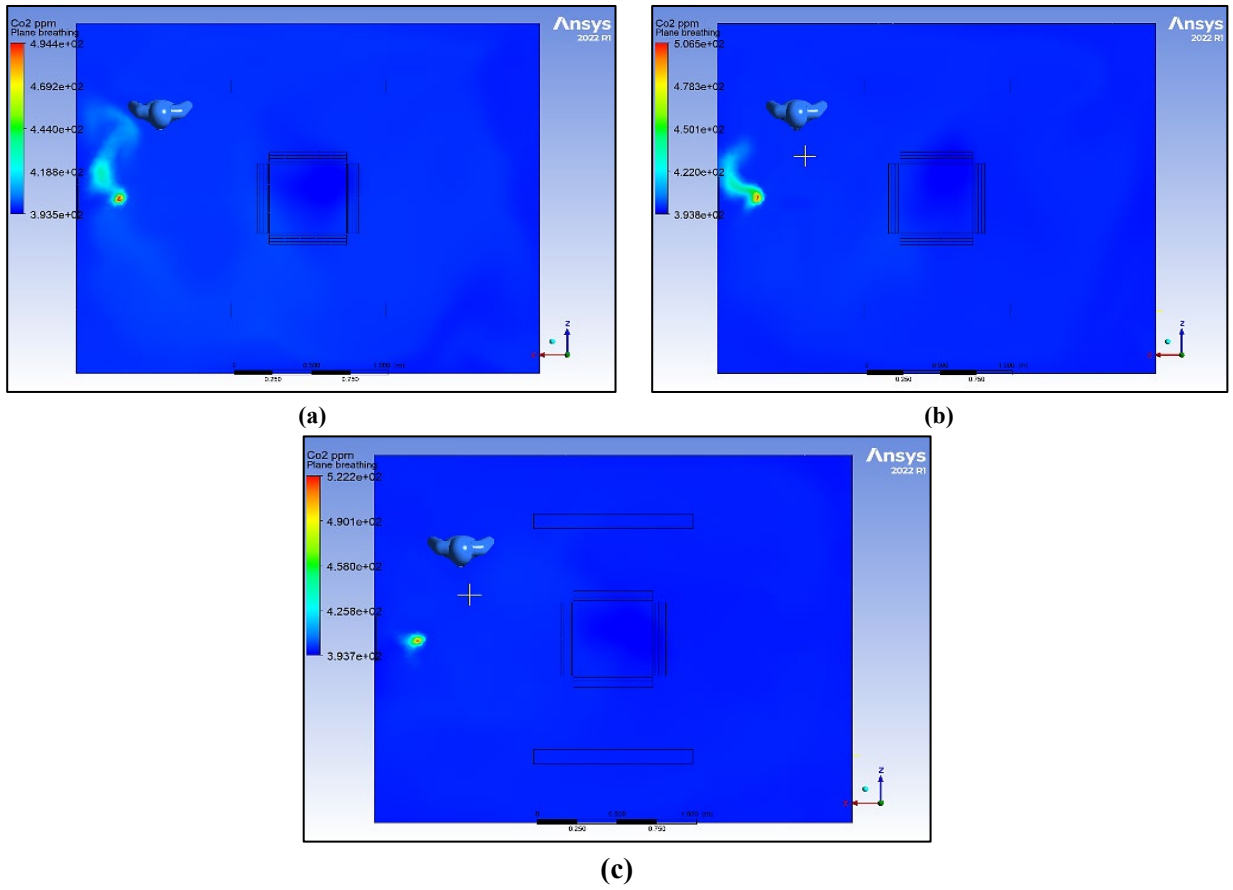


Figure 10: Illustration of a top-view breathing contaminant distribution at the breathing zone at 15 degrees. AC inclination angle at three different inlet speeds: (a) low speed, (b) medium speed, and (c) high speed

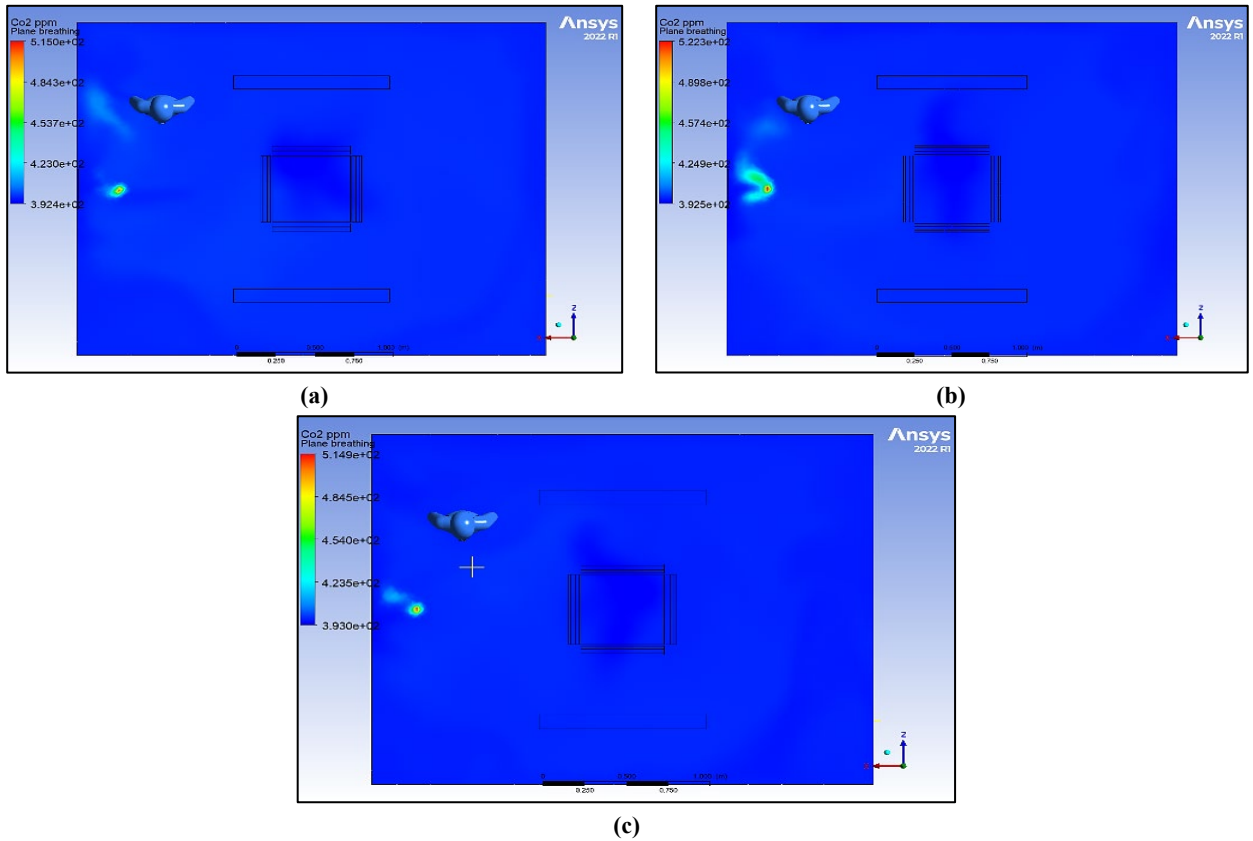


Figure 11: Illustration of a top view of breathing contaminant distribution at the breathing zone at 30 degrees. AC inclination angle at three different inlet speeds: (a) low speed, (b) medium speed, and (c) high speed

3.2 Contaminant removal index (CRE) result

Figure 12 indicates that the illustrations of a chart of the CRE of the present work at three different AC inclination angles and three different inlet velocities. The results suggest that setting the AC units at a 15-degree inclination optimizes the airflow patterns and ventilation effectiveness, leading to better removal of airborne contaminants, which reach 99.99% in high-speed mode, which is the maximum. In contrast, the 30-degree and 0-degree angles may result in suboptimal air circulation and pollutant removal, potentially leading to less effective indoor air quality improvement, which reached 99.91% and 98.1%, respectively, at high-speed mode in the overall three minutes.

These findings highlight the importance of considering the AC inlet angle as a critical factor in achieving better indoor air quality and controlling airborne contaminants. Setting the AC units at an inclination of 15 degrees appears to be the most effective engineering measure for improving the removal efficiency of contaminants in the indoor environment.

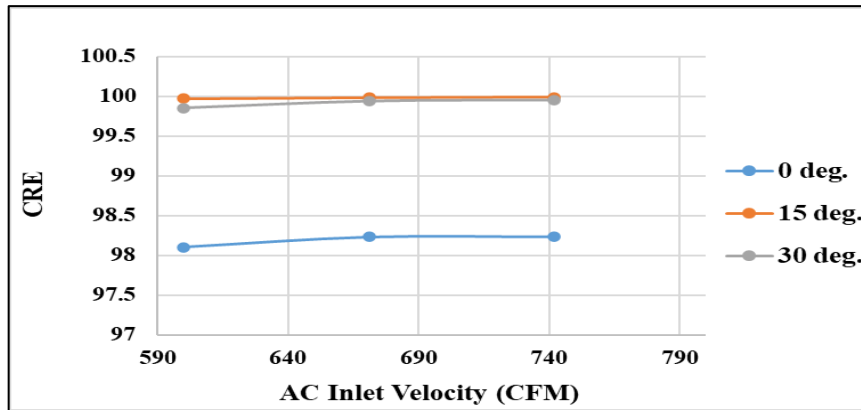


Figure 12: Illustrations of a chart of the CRE of the present work at three different AC inclination angles and three different AC inlet velocities

3.3 Local air quality index result

Figure 13 shows a Local Air Quality Index chart with inlet AC velocity at three different angles (0°, 15° and 30°). Showing values greater than one at a 15-degree inclination of the air conditioner (AC) inlet angle and values less than one for the zero and 30-degree angles suggests that the AC system's performance in terms of air quality improvement varies with the angle of the AC inlet. At the 15-degree inclination, the higher LAQI value indicates that the AC system's ventilation capabilities at negative pressure are more effective in reducing airborne contaminants and improving the local air quality. The inclined angle might facilitate better air circulation and capture of pollutants, resulting in a higher removal efficiency. In contrast, the lower LAQI values at the zero and 30-degree angles suggest a relatively reduced ability of the AC system to mitigate airborne contaminants. The straight or less inclined AC inlet angles may not promote optimal air mixing and pollutant removal, leading to lower efficiency in improving air quality. These findings highlight the significance of AC inlet angle in influencing air quality improvement. Optimizing the AC system's angle can enhance its performance in mitigating airborne contaminants and improving the local air quality. This could involve adjusting the AC unit's position or utilizing design modifications to optimize airflow patterns and increase contaminant removal efficiency.

The results obtained from this study provide valuable insights for designing and optimizing AC systems in various indoor environments, particularly those where air quality is a concern. They emphasize the importance of considering the AC inlet angle as a parameter to enhance air quality management strategies, ensuring healthier indoor environments for occupants. Additionally, assessing the impact of AC inlet angle on energy consumption, thermal comfort, and overall system performance would provide a comprehensive understanding of its implications in indoor air quality management.

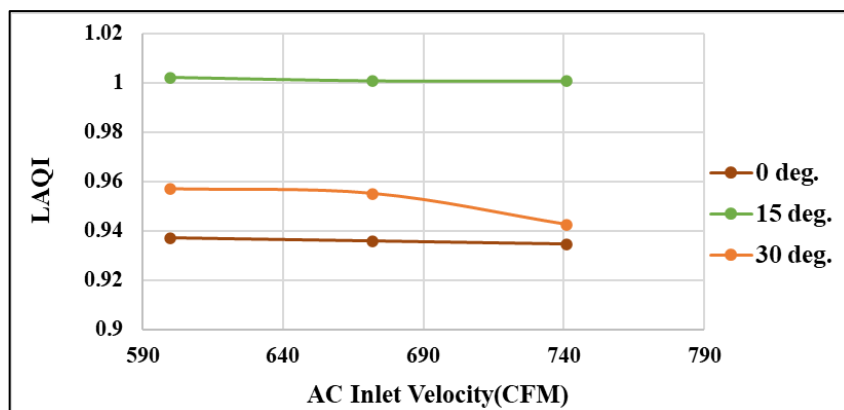


Figure 13: Illustrations of a chart of the LAQI of the present work at three different AC inclination angles and inlet velocities

3.4 Validation

The results of the current study are validated by comparison with the numerical study of [45] and the current numerical study at zero AC angle at 7.5 L/S.P, as shown in Figure 14. The Local ventilation effectiveness between the two sets of results was evaluated, as described in Figure 14. The agreement between the two studies' solutions was found to be satisfactory.

This difference may be attributed to factors such as the assumptions made in the numerical model and the precision of boundary conditions employed in the simulations. However, between the two studies, the maximum and minimum discrepancies were about (1-6)% respectively.

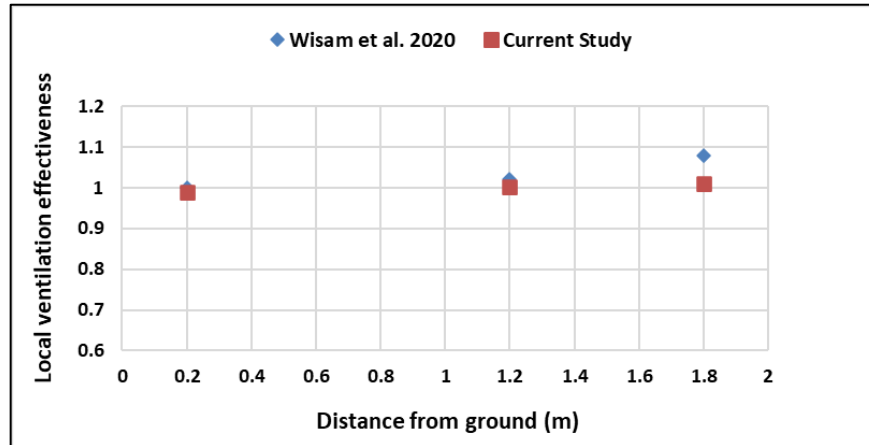


Figure 14: Comparison of current numerical results with Mareed study

4. Conclusion

From the previous findings of the present paper and the numerical results of CFD and according to the Coefficient of Removal Efficiency and Local Air Quality Index of Airborne Isolation Indoor Room at three different Air Conditioner angles and three different inlet air speeds, the following can summarize the conclusion of our study:

- 1) The CO₂ concentration was higher when the four cassette AC units were set at a 0-degree angle compared to inclinations of 15 and 30 degrees.
- 2) A 0-degree angle may result in localized stagnant air pockets, hindering the dilution and dispersion of CO₂ and leading to higher concentrations near the AC units. In contrast, inclinations of 15 and 30 degrees promote better air circulation, facilitating more efficient dilution and dispersion of CO₂.
- 3) The Coefficient of Removal Efficiency at the 15-degree inclination of the air conditioner inlet angle demonstrates the highest removal efficiency for contaminants, making it the most effective angle for improving indoor air quality.
- 4) The conclusion based on the Local Air Quality Index analysis is that the LAQI values indicate higher air quality at the 15-degree inclination of the air conditioner inlet angle compared to the 30-degree and 0-degree angles, making the 15-degree inclination the most favorable for achieving better indoor air quality.
- 5) The findings emphasize the importance of selecting appropriate AC inlet angles as an engineering control measure to safeguard the safety and well-being of medical staff. Implementing the 15-degree inclination helps maintain a safer working environment, protecting healthcare workers from airborne contamination and ensuring the containment of potential infections within the isolation rooms.

Finally, AC inlet angle on energy consumption, thermal comfort, and overall system performance would provide a comprehensive understanding of its implications in indoor air quality management.

Author contributions

Conceptualization, E. Barrak, H. Hussain and L. Habeeb; writing—review and editing, H. Hussain and L. Habeeb; supervision, H. Hussain, L. Habeeb; project administration, H. Hussain, L. Habeeb. All authors have read and agreed to the published version of the manuscript.

Funding

This research received no specific grant from any funding agency in the public, commercial, or not-for-profit sectors.

Data availability statement

Not applicable

Conflicts of interest

The authors of the current work do not have conflict of interest

References

- [1] ASHRAE, 2010. Guideline 10P, Interactions Affecting the Achievement of Acceptable Indoor Environments, Second Public Review. ASHRAE.

- [2] Organization, W.H., 2022. WHO Director-General's opening remarks at the Public Hearing regarding a new international instrument on pandemic preparedness and response – 12 April 2022.
- [3] A. S. Jaber, A. K. Hussein, N. A. Kadhim, and A. A. Bojassim, A Moran's I autocorrelation and spatial cluster analysis for identifying Coronavirus disease COVID-19 in Iraq using GIS approach, *Casp. J. Environ., Sci.*, 20 (2022) 55–60. <https://doi.org/10.22124/CJES.2022.5392>
- [4] Carlson, C.J., Albery, G.F., Merow, C., Trisos, C.H., Zipfel, C.M., Eskew, E.A., Olival, K.J., Ross, N., Bansal, S., 2022. Climate change increases cross-species viral transmission risk. *Nature*.
- [5] S. L. Pan, M. Cui, and J. Qian, Information resource orchestration during the COVID-19 pandemic: A study of community lockdowns in China, *Int. J. Inf. Manage.*, 54 (2020) 102143 <https://doi.org/10.1016/j.ijinfomgt.2020.102143>
- [6] G. Lin et al., Community evidence of severe acute respiratory syndrome coronavirus 2 (SARS-CoV-2) transmission through air, *Atmos Environ.*, 246 (2021) 118083. <https://doi.org/10.1016/j.atmosenv.2020.118083>
- [7] O. Fawwaz Alrebi, B. Obeidat, I. Atef Abdallah, E. F. Darwish, and A. Amhamed, Airflow dynamics in an emergency department: A CFD simulation study to analyse COVID-19 dispersion, *Alex. Eng. J.*, 61 (2022) 3435–3445. <https://doi.org/10.1016/j.aej.2021.08.062>
- [8] Y. al horr, M. Arif, M. Katafygiotou, A. Mazroei, A. Kaushik, and E. Elsarrag, Impact of indoor environmental quality on occupant well-being and comfort: A review of the literature, *Int. J. Sustainable Built Environ.*, 5 (2016) 1–11. <https://doi.org/10.1016/j.ijsbe.2016.03.006>
- [9] G. Cao, P. V. Nielsen, R. L. Jensen, P. Heiselberg, L. Liu, and J. Heikkinen, Protected zone ventilation and reduced personal exposure to airborne cross-infection, *Indoor Air*, 25 (2015) 307–319. <https://doi.org/10.1111/ina.12142>
- [10] P. Kumar and L. Morawska, Could fighting airborne transmission be the next line of defence against COVID-19 spread?, *City Environ. Interact.*, 4 (2019) 100033 <https://doi.org/10.1016/j.cacint.2020.100033>
- [11] S. L. Pan, M. Cui, and J. Qian, Information resource orchestration during the COVID-19 pandemic: A study of community lockdowns in China, *Int. J. Inf. Manage.*, 54 (2020) 102143. <https://doi.org/10.1016/j.ijinfomgt.2020.102143>
- [12] Z. D. Bolashikov and A. K. Melikov, Methods for air cleaning and protection of building occupants from airborne pathogens, *Build. Environ.*, 44 (2009) 1378–1385. <https://doi.org/10.1016/j.buildenv.2008.09.001>
- [13] L. Morawska, Droplet fate in indoor environments, or can we prevent the spread of infection?, in *Indoor Air*, Oct. 16 (2006) 335–347. <https://doi.org/10.1111/j.1600-0668.2006.00432.x>
- [14] T. T. Chow, A. Kwan, Z. Lin, and W. Bai, A computer evaluation of ventilation performance in a negative-pressure operating theater, *Anesth Analg*, 103 (2006) 913–918. <https://doi.org/10.1213/01.ane.0000237404.60614.24>
- [15] D. G. Karottki et al., An indoor air filtration study in homes of elderly: cardiovascular and respiratory effects of exposure to particulate matter, 2013. <https://doi.org/10.1186/1476-069x-12-116>
- [16] H. C. Chuang, L. Y. Lin, Y. W. Hsu, C. M. Ma, and K. J. Chuang, In-car particles and cardiovascular health: An air conditioning-based intervention study, *Sci. Total Environ.*, 452–453 (2013) 309–313. <https://doi.org/10.1016/j.scitotenv.2013.02.097>
- [17] S. Liu, G. Cao, B. E. Boor, and A. Novoselac, A Protected Occupied Zone Ventilation System to Prevent the Transmission of Coughed Particles.
- [18] O. Bamodu, L. Xia, and L. Tang, A Numerical Simulation of Air Distribution in an Office Room Ventilated by 4-Way Cassette Air-conditioner, *Energy Procedia*, 105 (2017) 2506–2511. <https://doi.org/10.1016/j.egypro.2017.03.722>
- [19] D. Al Assaad, K. Ghali, and N. Ghaddar, Effectiveness of intermittent personalized ventilation assisting a chilled ceiling for enhanced thermal comfort and acceptable indoor air quality, *Build Environ.*, 144 (2018) 9–22. <https://doi.org/10.1016/j.buildenv.2018.08.005>
- [20] G. Cao, M. C. A. Storås, A. Aganovic, L. I. Stenstad, and J. G. Skogås, Do surgeons and surgical facilities disturb the clean air distribution close to a surgical patient in an orthopedic operating room with laminar airflow?, *Am J. Infect Control*, 46 (2018) 1115–1122. <https://doi.org/10.1016/j.ajic.2018.03.019>
- [21] J. Cho, Investigation on the contaminant distribution with improved ventilation system in hospital isolation rooms: Effect of supply and exhaust air diffuser configurations, *Appl. Therm. Eng.*, 148 (2019) 208–218. <https://doi.org/10.1016/j.applthermaleng.2018.11.023>
- [22] Y. Zhang et al., Adaptive Wall-Based Attachment Ventilation: A Comparative Study on Its Effectiveness in Airborne Infection Isolation Rooms with Negative Pressure, *Eng.*, 8 (2022) 130–137. <https://doi.org/10.1016/j.eng.2020.10.020>
- [23] S. ALJABAIR, I. ALESBE, and A. ALKHALAF, CFD modeling of influenza virus diffusion during coughing and breathing in a ventilated room, *J. Therm. Eng.*, 9 (2023) 127–137. <https://doi.org/10.18186/thermal.1243491>
- [24] M. Alkhalaf, A. Ilinca, and M. Y. Hayyani, CFD Investigation of Ventilation Strategies to Remove Contaminants from a Hospital Room, *Designs (Basel)*, 7 (2023) <https://doi.org/10.3390/designs7010005>

- [25] <https://chigo.bgenproductcassette-type-air-conditioner-chigo-cca-24-hvr1-23000-btu-hvr1>.
- [26] T. T. Chow, A. Kwan, Z. Lin, and W. Bai, Conversion of operating theatre from positive to negative pressure environment, *J. Hosp. Infect.*, 64 (2006) 371–378. <https://doi.org/10.1016/j.jhin.2006.07.020>
- [27] J.-M. Huang and S.-M. Tsao, The Influence of Air Motion on Bacteria Removal in Negative Pressure Isolation Rooms. *HVAC & R. Research*, 11(2005) 563-585. <https://doi.org/10.1080/10789669.2005.10391155>
- [28] M. Hajdukiewicz, M. Geron, and M. M. Keane, “Calibrated CFD simulation to evaluate thermal comfort in a highly-glazed naturally ventilated room,” *Build Environ*, 70(2013)73–89. <https://doi.org/10.1016/j.buildenv.2013.08.020>
- [29] M. Bivolarova, J. Ondráček, A. Melikov, and V. Ždímal, A comparison between tracer gas and aerosol particles distribution indoors: The impact of ventilation rate, interaction of airflows, and presence of objects, *Indoor Air*, 27 (2017) 1201–1212. <https://doi.org/10.1111/ina.12388>
- [30] Y. Bi, A. Aganovic, H. M. Mathisen, and G. Cao, Experimental study on the exposure level of surgical staff to SARS-CoV-2 in operating rooms with mixing ventilation under negative pressure, *Build. Environ.*, 217 (2022)109091. <https://doi.org/10.1016/j.buildenv.2022.109091>
- [31] H. A. Olvera, A. R. Choudhuri, and W. W. Li, Effects of plume buoyancy and momentum on the near-wake flow structure and dispersion behind an idealized building, *J. Wind Eng. Ind. Aerodyn.*, 96 (2008) 209–228. <https://doi.org/10.1016/j.jweia.2007.04.004>
- [32] Y. Tominaga et al., AIJ guidelines for practical applications of CFD to pedestrian wind environment around buildings, *J. Wind Eng. Ind. Aerodyn.*, 96 (2008) 1749–1761. <https://doi.org/10.1016/j.jweia.2008.02.058>
- [33] M. Lateb, C. Masson, T. Stathopoulos, and C. Bédard, Simulation of near-field dispersion of pollutants using detached-eddy simulation, *Comput. Fluids.*, 100 (2014) 308–320. <https://doi.org/10.1016/j.compfluid.2014.05.024>
- [34] Y. Lu, M. Oladokun, and Z. Lin, Reducing the exposure risk in hospital wards by applying stratum ventilation system, *Build. Environ.*, 183 (2020) 107204. <https://doi.org/10.1016/j.buildenv.2020.107204>
- [35] Y. Tao, K. Inthavong, and J. Y. Tu, Dynamic meshing modelling for particle resuspension caused by swinging manikin motion, *Build. Environ.*, 123 (2017) 529–542. <https://doi.org/10.1016/j.buildenv.2017.07.026>
- [36] A. Aganovic, M. Steffensen, and G. Cao, CFD study of the air distribution and occupant draught sensation in a patient ward equipped with protected zone ventilation, *Build. Environ.*, 162 (2019) 106279. <https://doi.org/10.1016/j.buildenv.2019.106279>
- [37] D. al Assaad, C. Habchi, K. Ghali, and N. Ghaddar, Effectiveness of intermittent personalized ventilation in protecting occupant from indoor particles, *Build. Environ.*, 128 (2018) 22–32. <https://doi.org/10.1016/j.buildenv.2017.11.027>
- [38] ANSYS Fluent Theory Guide, 2015. [Online]. Available: <http://www.ansys.com>
- [39] F. A. Berlanga, M. R. de Adana, I. Olmedo, J. M. Villafruela, J. F. San José, and F. Castro, Experimental evaluation of thermal comfort, ventilation performance indices and exposure to airborne contaminant in an airborne infection isolation room equipped with a displacement air distribution system, *Energy Build.*, 158 (2018) 209–221. <https://doi.org/10.1016/j.enbuild.2017.09.100>
- [40] Z. Cheng, A. Aganovic, G. Cao, and Z. Bu, Experimental and simulated evaluations of airborne contaminant exposure in a room with a modified localized laminar airflow system, *Environ. Sci. Pollut. Res.*, 28 (2021) 30642–30663. <https://doi.org/10.1007/s11356-021-12685-4>
- [41] S. Zhang, D. Niu, Y. Lu, and Z. Lin, Contaminant removal and contaminant dispersion of air distribution for overall and local airborne infection risk controls, *Sci. Total Environ.*, 833 (2022) 155173. <https://doi.org/10.1016/j.scitotenv.2022.155173>
- [42] Z. Liu et al., A novel design strategy to interrupt the diffusion of exhaled aerosols: an 2 integrated experimental-numerical investigation. <https://doi.org/10.2139/ssrn.4166072>
- [43] Olmedo, P. V. Nielsen, M. Ruiz de Adana, R. L. Jensen, and P. Grzelecki, Distribution of exhaled contaminants and personal exposure in a room using three different air distribution strategies, *Indoor Air*, 22 (2012) 64–76. <https://doi.org/10.1111/j.1600-0668.2011.00736.x>
- [44] . Ameer, A. Azmi, N. Normunira, M. Hassan, and Z. M. Salleh, Investigation of Airflow in A Restaurant to Prevent COVID-19 Transmission Using CFD Software MALAYSIA *Corresponding Author Designation, *Eng. Appl. Technol.*, 3 (2021) 977–991. <https://doi.org/10.30880/peat.2022.03.01.095>
- [45] W. Mareed and H. Hussen, Numerical and Experimental Modeling of Indoor Air Quality Inside a Conditioned Space with Mechanical Ventilation and DX-Air Conditioner, *Eng. Technol. J.*, 38 (2020) 1257–1275. <https://doi.org/10.30684/etj.v38i9A.875>